

ChemComm

Accepted Manuscript



This is an *Accepted Manuscript*, which has been through the Royal Society of Chemistry peer review process and has been accepted for publication.

Accepted Manuscripts are published online shortly after acceptance, before technical editing, formatting and proof reading. Using this free service, authors can make their results available to the community, in citable form, before we publish the edited article. We will replace this *Accepted Manuscript* with the edited and formatted *Advance Article* as soon as it is available.

You can find more information about *Accepted Manuscripts* in the [Information for Authors](#).

Please note that technical editing may introduce minor changes to the text and/or graphics, which may alter content. The journal's standard [Terms & Conditions](#) and the [Ethical guidelines](#) still apply. In no event shall the Royal Society of Chemistry be held responsible for any errors or omissions in this *Accepted Manuscript* or any consequences arising from the use of any information it contains.

Simultaneous Synthesis/Assembly of Anisotropic Cake-shaped Porphyrin Particles toward Colloidal Microcrystals

Received 00th January 20xx,
Accepted 00th January 20xx

Ting Wang,^{†a} Minxuan Kuang,^{†b} Feng Jin,^b Jinhua Cai,^c Lei Shi,^d Yongmei Zheng^a, Jingxia Wang,^{*b} and Lei Jiang^b

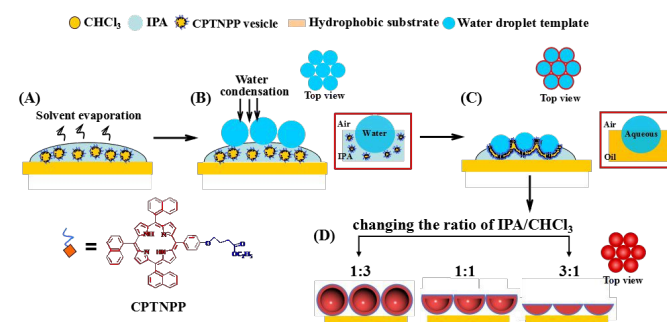
DOI: 10.1039/x0xx00000x

www.rsc.org/

One-step synthesis/assembly of cake-shaped porphyrin colloidal microcrystal with tailored height-diameter was demonstrated based on the interfacial assembly and water-droplet template. The as-fabricated anisotropic colloidal crystals showed special optic property and enhanced optic-limiting behavior.

Anisotropic particles and the corresponding colloidal crystals (CCs)¹⁻⁵ have attracted wide research interest because of their promising applications^{1c} in optic^{1b,4} sensing device^{2a} and separation films.^{2c} Typically, simple shape anisotropy has the potential to construct the assembly structure that is infeasible for spherical particles. The full-bandgap CCs can be expected since shape^{6a} or dielectrically anisotropic^{6b} may break the degeneracy resulting from symmetry at the W- or U-point of the band structure.⁶ However, it is extremely difficult to control the orientation of anisotropic particles during the assembly process and in the final crystals by just convective assembly.⁷⁻⁸ Accordingly, some additional assembly forces, such as electronic⁹, magnetic fields¹⁰ or interfacial interaction¹¹ have been introduced to induce the orientated arrangement of the anisotropic particles. For example, Song^{10a} and Yin^{10b-c} attained iridescent CCs from Fe₂O₃/SiO₂ particles in a magnetic field. Furst *et al.* realized ellipsoidal colloidal assembly by electric filed⁹, that induced polarization/assembly of the colloidal particles in dipolar interactions. There remains a great challenge to develop a facile approach for the fabrication of anisotropic CCs, which is of great significance for the creation of novel and advanced optic materials/devices. Recently, interface tension-induction has become an effective approach for the preparation of various functional anisotropic

particles.¹² Series of anisotropic mesoporous hollow spheres were fabricated from interface-induced shrinkage/encapsulation interaction^{12b-c}. Combining the interface-induced and spontaneous formation/arrangement of water-droplet template,¹³ we fabricated morphology-controlled anisotropic porphyrin particles^{14a} and the well-ordered arrangement of flower-shaped porphyrin particles^{14b}. In this paper, we further extended the approach for the one-step construction of anisotropic porphyrin CCs assembled from cake-shaped particles based on the interfacial encapsulation of droplet template by porphyrin suspension. The ratio of the height and diameter (H/D) of cake-shaped particles can be meticulously modulated from 1 to 0.33 by changing the composition of porphyrin suspension, which affects the optic properties such as reflection spectrum and the optical limiting effect of the as-prepared porphyrin CCs. This facile approach will offer significant insight for the design and fabrication of anisotropic CCs, which would be of great importance for the extended applications of the anisotropic CCs in various optic devices.



Scheme 1. Illustration of the formation process of anisotropic porphyrin CCs from cake-shaped particles. The process includes spreading the porphyrin suspension onto the substrate (A, B), condensation of the droplet template at the interface of air-suspension (C), encapsulation of the porphyrin vesicles around the droplet (D), and the formation of cake-shaped CCs (E). Distinct anisotropic CCs were produced owing to different solvent fractions in CPTNPP suspension. The chemical structure of CPTNPP is inserted.

Scheme 1 presents the one-step formation process of anisotropic CCs assembled from cake-shaped particles of porphyrin derivative of 5-(4-(ethylcarboxypropoxy)phenyl)-10,15,20-tri(naphthyl) porphyrin (CPTNPP). Here, the selection

^aSchool of Chem & Environm, Beihang University, Beijing 100191, P. R. China

^bLaboratory of Bio-Inspired Smart Interface Sciences, Technical Institute of Physics and Chemistry, Chinese Academy of Sciences, Beijing 100190, P. R. China

Corresponding E-mail: jingxiawang@mail.ipc.ac.cn, wangzhang@iccas.ac.cn

^cCollege of Chemistry & Chemical Engineering, Jinggangshan University, Jian, Jiangxi Province 340039, P. R. China

^dDepartment of Physics, Key Laboratory of Micro & Nano Photonic Structures (MOE) and Key Laboratory of Surface Physics, Fudan University, Shanghai 200433, P. R. China

[†] T. Wang and M. X. Kuang contribute equal to this article.

Electronic Supplementary Information (ESI) includes the morphology of the anisotropic CCs, the formation process, and the UV-vis reflection spectra is available. See DOI: 10.1039/x0xx00000x

of porphyrin derivative is mainly due to the peculiar optoelectronic property based on the unique planar, rigid molecular geometry¹⁵, which may produce potential applications¹⁵ in optic-limit¹⁶, optic catalytic and etc. Firstly, the CPTNPP suspension is prepared (scheme 1A) by dispersing a chloroform solution of CPTNPP ($10^{-5} \sim 10^{-6}$ mol/L) into isopropyl alcohol (IPA) with certain volume fraction, followed by spreading the CPTNPP suspension onto the substrate (Scheme 1B). Subsequently, the water droplet would condensate and assembly at the interface of air-dispersion induced by the solvent evaporation (Scheme 1C). After the encapsulation of the water droplet by CPTNPP vesicles accompanied with solvent evaporation (Scheme 1D), the anisotropic CCs were produced (Scheme 1E). Meantime, these anisotropic particles can be homogeneously oriented and assembly at the interface of air- IPA suspension. Notably, the shape of particles can be effectively modulated from spherical- to hemispherical- or even slice-like structure by varying the solvent fraction in CPTNPP suspension.

Figure 1 demonstrates SEM images of as-fabricated anisotropic CCs from changing the IPA fraction in the CPTNPP suspension (more detailed data can be found in SEM and AFM images in Figure S4-S8). Clearly, the shape of as-fabricated particles were meticulously tuned from a whole hollow-sphere (Figure 1A) to semi-sphere (Figure 1B, C, E) or even solid slice-like (Figure 1D, F) structure when increasing the IPA fraction in the CPTNPP suspension from 25%, to 33.3%, to 50%, to 66.7% respectively, accompanied with a decrease of H/D for cake-shaped particles from 1, to 0.8, to 0.6, and to 0.33. As-obtained particles exhibited a shrinkable cavity structure corresponding to the decreased H/D that can be clearly observed from inserted TEM images and illustrated cross-section scheme in the upper right corner in Figure 1(A-D). At first, the as-prepared particles are perfect hollow spheres with diameter of $2.25 \pm 0.09 \mu\text{m}$ and homogeneous shell thickness of 200 nm in Figure 1A. Subsequently, the particles gradually turn to be hemi-spheres with height of about 2.1 μm and 1.5 μm respectively, which have a decreased hollow cavities (in Figure 1B and 1C). Finally, solid slice-like particles can be obtained with height of 500 nm and H/D of 0.33. The solid structure of slice-like particles can be clearly proved from TEM images in Figure 1D and SEM images in Figure 1F and S7B. The diameters of as-obtained particles are summarized in Figure S9.

Importantly, the as-prepared anisotropic particles showed well-ordered arrangement regardless of its shape alteration. As shown in Figure 1A-D, the colloidal particles exhibited a clear and close-packed face-centered cubic structure, with a homogeneously orientation arrangement, i.e., with its spherical side toward the substrate, and the flat one toward the air as shown in Figure 1E and 1F. The homogeneously oriented arrangement of the anisotropic particles can be attributed to a simultaneous formation and assembly of the anisotropic particles at one step. Concretely, the droplet template spontaneously formed and assembly in the interface of air/CPTNPP suspension in well-ordered way (Scheme 1C). Wherein, one end of drop is immersed in CPTNPP vesicles toward the formation of spheric end, while the exposed part is

encapsulated toward the formation of flat side. As a result, a well-ordered droplet template array turns to be close-packed anisotropic CCs, keeping the similar orientation arrangement. Wherein, the H/D of particles can be modulated by varying the composition of CPTNPP suspension.

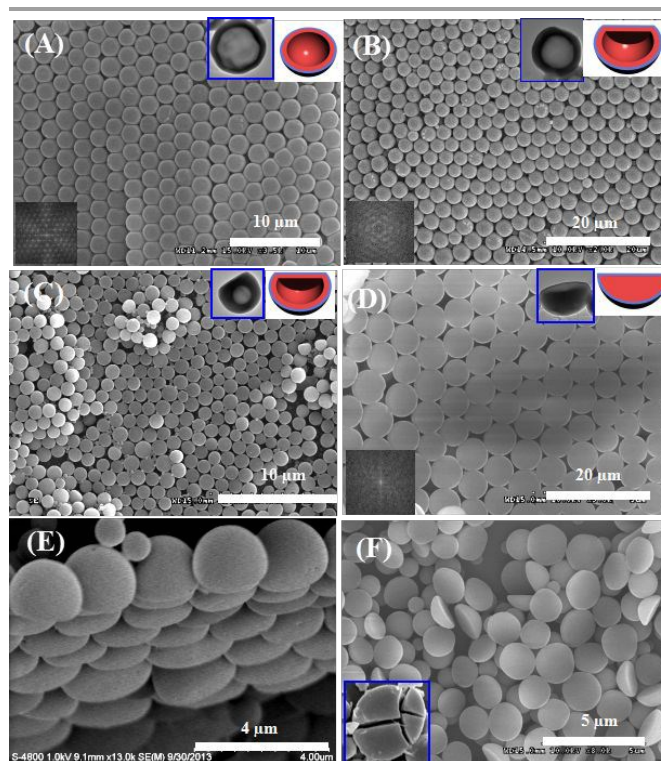


Figure 1. SEM images of as-prepared anisotropic porphyrin CCs from cake-shaped particles prepared from different IPA fraction in the porphyrin suspension. The lower left and upper right corner in (A), (B), (C) and (D) are the FFT transfer (of the corresponding SEM image of as-prepared CCs) and TEM images of particles respectively, indicating the well-ordered arrangement of CCs from particles with decreased H/D in (A) 1, to (B) 0.8, to (C, E) 0.6 and to (D, F) 0.33.

Figure 2A-C schemes the possible formation process of anisotropic particles and its tunable shape resulted from the various CPTNPP suspension. After the water droplets are condensed onto the surface of the CPTNPP suspension, it adopts a conformation determined by the surface tension and interfacial tension of H_2O and CPTNPP suspension. Accompanied with the solvent evaporation, the porphyrin vesicles encapsulated around the immersed part of water droplet template as shown in Figure 2B, resulting in the formation of the cake-shaped particles in Figure 2C. In this case, the shape of the as-prepared particles is defined by the contact angle (CA, θ_c) of the immersed critical water droplet, formed by the intersection of the water droplet, CPTNPP suspension and air interface. θ_c can be predicted by the modified Young's equation^{17a,b} as shown in Figure 3C, the detailed induction process of this equation is in the Figure S10-12 and Table S1-S3.

$$\cos \theta_c = \frac{\gamma_{g-l_o} - \gamma_{g-l_w}}{\gamma_{l_w-l_o}}$$

Wherein, l_w is aqueous phase, l_o is oil phase. (Here, we neglect the effect of CPTNPP on the system to simplify the calculation). γ_{g-l_w} and γ_{g-l_o} are the surface tension of aqueous phase and oil

ChemComm

phase in air respectively. γ_{lv-lo} is the interface tension of aqueous/oil. In our case, the aqueous phase is the H₂O mixing of IPA with varying fraction from 0 to 60%, and the oil phase is the chloroform mixing of IPA with varying fraction from 0 to 60%. The surface tension and interfacial tension of the as-formulated liquids are determined by the shape of pendant liquid droplet in air or liquid^{17c} respectively. The experimental data are presented in Table S2 and S3. Figure 2D schemes the relationship between H/D and θ_c ($H/D = 0.5 \cdot (1 - \cos\theta_c)$). H/D falls with the decrease of θ_c .

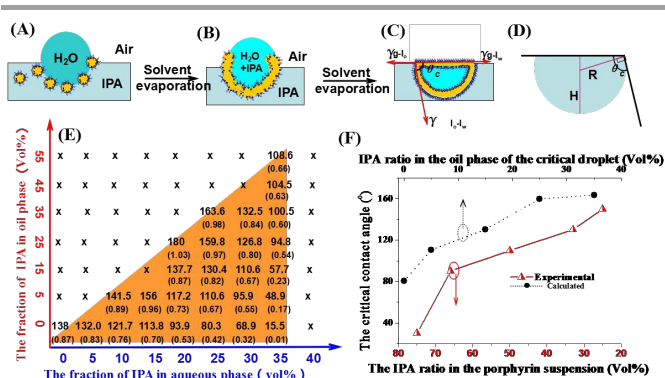


Figure 2. (A-C) Illustration of the morphological evolution process for the water droplet template. (A) The water droplet template formed on the porphyrin suspension, (B) Water droplet encapsulated by porphyrin vesicles, (C) Critical water droplet encapsulated by the oil layer of porphyrin suspension, (D) scheme for the relationship between H/D and the θ_c . (E) The calculated θ_c (H/D) when varying IPA fraction in the oil/aqueous phase. (F) Theoretical (black curve) and experimental (red curve) of θ_c when varying IPA fraction in the oil phase.

Figure 2E exhibits the calculated θ_c (H/D) of the corresponding aqueous droplet encapsulated by oily layer using **Equation 1**. The calculation equation of the ratio of H/D can be found in Figure S10. Clearly, there was an obvious fall in θ_c when decreasing the IPA fraction in oily layer encapsulated of the critical droplet. For example, θ_c drops from 163°, to 159°, to 130.4°, to 110.6°, to 80.26°, and H/D fell from 0.98, to 0.82, to 0.67, and to 0.42 when the IPA fraction in oily layer encapsulated of the critical droplet was decreased from 35%, to 25%, to 15%, and to 5% as shown by black curve in Figure 2F. Unexpectedly, a seemingly contradictory changing trend is observed for the experimental values of θ_c (red solid line in Figure 2F). Concretely, θ_c rises from 30° to 150°, and H/D climbs from 0.15 to 1 when the IPA fraction in porphyrin suspension dropped from 80% to 20%. That is, an increased IPA fraction in the porphyrin suspension (for the feeding formula) resulted in a decreased IPA fraction in the oily layer of the critical droplet. This seemingly contrary changing trend mainly can be attributed to IPA effect on evaporation rate by varying spreading area (the CA of the initial droplet). Wherein, an increased IPA dosage in porphyrin suspension would result in a decreased water CA on the substrate (Table S4), which effectively accelerates the evaporation of the IPA, remaining less fraction of IPA in the critical water droplet.^{14a} Thus, an increased fraction of IPA in the CPTNPP suspension (initial droplet) implies a decreased retaining of IPA in the critical droplet.^{16d} Accordingly, the predicted changing trend of the dimension for cake-shaped particles shown in Figure 3F is in

consistent with the experimental observation. By precisely manipulating θ_c based on varying the IPA fraction in CPTNPP suspension, the vesicle suspension allows for the synthesis of cake-shaped particles with controllable height. It should be mentioned that the shrinkable cavity structure can be attributed to the decreased immersion of water droplet in the suspension resulted from the decreasing IPA fraction, which restricts the assembly and aggregation of the porphyrin vesicles, leading to the resultant solid- slice structure in Figure 1D, F.

Besides the tailored morphology of the particles, the as-fabricated colloids demonstrated specific optic properties aroused from the well-ordered arrangement of the cake-shaped particles in **Figure 3**. Figure 3A shows a distinct reflection signal at ca. 6.5 μm . It is different from smooth reflection spectra of the common CCs: some striking wavy structures decorated the spectra of the as-fabricated samples. These wavy structures could be assigned to the corresponding chemical signal of CPTNPP in the infrared spectra of the smooth CPTNPP film, such as carboxy group (1732 cm^{-1}), ester or ether group (1249, 1177 cm^{-1}), and aromatic porphyrin group (1500, 1473 cm^{-1}). That is, the as-obtained reflection spectra of cake-shaped CCs suggest compound information of the geometrical structure and chemical components. Furthermore, the reflection signal of as-fabricated 2-dimensional cake-shaped CCs shifted from 5.1, 7.0 to 9.2 μm when varying the value of H/D from 0.6, 0.8 to 1 in Figure 3B. These red-shifts of the spectra signal are in well agreement with the simulated result in dot line of Figure 3B from FDTD Solutions¹⁸: stopband shift from 5.1, to 6.5, to 7.5 μm with the increased H/D of cake-shaped particles. This implied an effective modulation of the optic properties for as-prepared porphyrin CCs by H/D. Intrinsically, the shift of the stopband is mainly aroused from the change of the height and refractive index of the particles based on the Bragg equation.¹⁸ In our case, the growth of the height plays a positive influence on the red-shift of the spectra although some modulation resulted from the refractive index owing to the varying cavity structure.

On the other hand, the as-prepared CPTNPP CCs showed nonlinear optical character. Nonlinear optical materials play an important role in the applications of signal processing, ultrafast optical communication and laser protection *etc.*¹⁶ Herein, we performed the nonlinear transmittance measurements to compare the optical limiting effects of CPTNPP CCs, smooth CPTNPP film and CPTNPP solution respectively. Optical limiting at 1064 nm was recorded using an Nd:YAG/optical parametric oscillator laser delivering 8 ns pulses for excitation. Figure 3C,D shows the curves of output fluence vs. input fluence for these samples. It is observed that the optical limiting threshold of CPTNPP CCs is approximately 1.7 J/cm^2 and 0.66 J/cm^2 for samples with H/D=0.6 and H/D=0.8, respectively, while little optic-limit phenomenon can be observed for the samples of CPTNPP solution and the smooth film. The improved optical limiting effects of CPTNPP CCs can be attributed to the highly ordered molecular aggregate in the CPTNPP CCs and the well-ordered latex arrangement. (The contrast experiment is found that little

optic limit property was observed for the sample when irradiated by 530 nm lasers). The well-ordered molecular aggregate of CPTNPP can be clearly confirmed from UV-Vis spectrum (Figure S3): the cake-shaped assemblies display a splitted blue-shifted Soret-band at *ca.* 391 nm (Figure S3) and part red-shifted Soret-band at 464 nm, combining with a relatively sharper profile at ~ 650 nm for CCs than that of the broad Q band of the monomeric CPTNPP. These suggested that most CPTNPPs therein is possibly organized as J-like aggregates,¹⁹ resulting in the formation of well-orientated aggregation for CPTNPPs: with the hydrophilic group toward the outside, while the hydrophobic porphyrin core toward the interior.^{14a} As can be further clarified in XPS result in Figure S2. All of these distinct aggregate mode contributes to the improved optic limiting property.

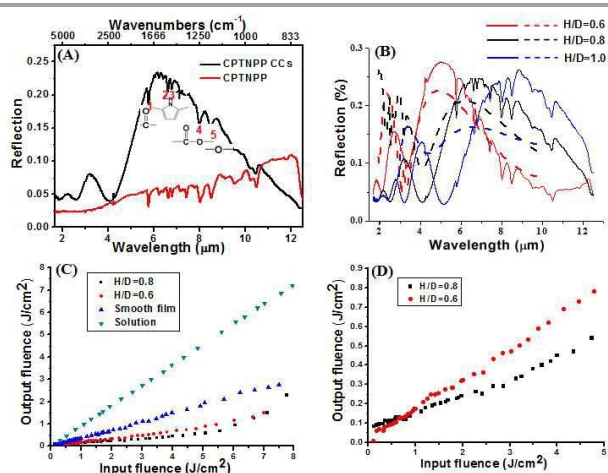


Figure 3. Optic properties of the as-prepared samples. (A) Comparative reflection signal of the CPTNPP CCs (dark line) and the smooth CPTNPP film (red line). The corresponding coordinate (cm^{-1}) and the typical chemical composition is noted. (B) The calculated (Solid line) and simulated (Dash line) reflection signal of the as-prepared CPTNPP CCs from cake-shaped particles with different H/D, the data is simulated from FDTD Solutions.¹⁷ (C) The curves of output fluence vs. input fluence for CPTNPP CCs, smooth CPTNPP film and CPTNPP solution. (D) Magnified curves of output fluence vs. input fluence for CPTNPP CCs.

In conclusion, a facile fabrication approach for the cake-shaped CCs is demonstrated based on droplet template and interface induction. The as-prepared samples demonstrate unique reflection signal in infrared region and enhanced optical limiting effects. This facile fabrication approach will provide an important insight for the creation and development of novel anisotropic CCs. It is also of great significance for the extended applications of functional materials such as porphyrin in novel optic-electric devices.

J. X. Wang would like to thank the NSFC (Grant No. 51373183, 51503214, 91127029, and 50973117) for the financial support.

Notes and references

- [1] (a) J. G. Park, J. D. Forster, E. R. Dufresne, *J. Am. Chem. Soc.* 2010, **132**, 5960; (b) T. Adachi, L. Tong, J. Kuwabara, T. Kanbara, A. Saeki, S. Seki, Y. Yamamoto, *J. Am. Chem. Soc.* 2013, **135**, 870; (c) B. Walther, A. H. E. Muller, *Chem. Rev.* 2013, **113**, 5194; (d) J. V. L. Timonen, M. Latikka, L. Leibler, R. H. A. Ras, O. Ikkala, *Science* 2013, **341**, 253.
- [2] (a) S.-H. Kim, A. D. Hollingsworth, S. Sacanna, S.-J. Chang, G. Lee, D. J. Pine, G.-R. Yi, *J. Am. Chem. Soc.* 2012, **134**, 16115; (b) W. Gao, A. Pei, X. M. Feng, C.

- Hennessy, J. Wang, *J. Am. Chem. Soc.* 2013, **135**, 998; (c) S. Fujii, M. Kappl, H. J. Butt, T. Sugimoto, Y. Nakamura, *Angew. Chem. Int. Ed.* 2012, **124**, 9947.
- [3] (a) J. T. Zhang, X. Chao, S. A. Asher, *J. Am. Chem. Soc.* 2013, **135**, 11397; (b) Y. Liu, C. Y. Yu, H. Jin, B. Jiang, X. Y. Zhu, Y. F. Zhou, Z. Y. Lu, D. Y. Yan, *J. Am. Chem. Soc.* 2013, **135**, 4765; (c) L. Fan, D. P. Josephson, A. Stein, *Angew. Chem. Int. Ed.* 2011, **50**, 360;
- [4](a) C. S. Huang, C. F. Xing, S. Wang, Y. J. Li, H. B. Liu, S. W. Lai, C. M. Che, Y. L. Li, *Chem. Commun.* 2011, **47**, 7644; (b) Z. Y. Yu, C. F. Wang, L. T. Ling, L. Chen, S. Chen, *Angew. Chem. Int. Ed.* 2012, **51**, 2375; (c) T. Q. Wang, X. Li, J. H. Zhang, X. Z. Wang, X. Z. Wang, X. M. Zhang, X. Zhang, D. F. Zhu, Y. D. Hao, Z. Y. Ren, B. Yang, *Langmuir* 2010, **26**, 13715.
- [5] (a) B. Ai, L. M. Wang, H. Mohwald, Y. Yu, G. Zhang, *Nanoscale* 2014, **6**, 8997; (b) S. W. Hsu, C. Ngo, A. R. Tao, *Nano Letters* 2014, **14**, 2372; T. Ding, F. Wang, K. Song, G. Q. Yang, C. H. Tung, *J. Am. Chem. Soc.* 2010, **132**, 17340.
- [6](a) J. W. Haus, H. S. Sozuer, R. Inguva, *J. Mod. Opt.* 1992, **39**, 1991; (b) Z. Y. Li, J. Wang, B. Y. Gu, *Phys. Rev. B* 1998, **58**, 3721.
- [7] (a) M. Fu, K. Chaudhary, J. G. Lange, H. S. Kim, J. J. Juarez, J. A. Lewis, P. V. Braun, *Adv. Mater.* 2014, **26**, 1740; (b) S. Y. Lee, S. Yang, *Angew. Chem. Int. Ed.* 2013, **52**, 8160; (b) D. Ershov, J. Sprakel, J. Appel, M. A. C. Stuart, J. van der Gucht, *PNAS* 2013, **110**, 9220; (c) S. Sacanna, M. Korpics, K. Rodriguez, L. Colon-Melendez, S. H. Kim, D. J. Pine, G. R. Yi, *Nat. Commun.* 2013, **4**, 1688.
- [8] (a) I. D. Hosein, C. M. Liddell, *Langmuir* 2007, **23**, 8810; (b) I. D. Hosein, S. H. Lee, C. M. Liddell, *Adv. Funct. Mater.* 2010, **20**, 3085; (c) S. Jiang, Q. Chen, M. Tripathy, E. Luijten, K. S. Schweizer, S. Granick, *Adv. Mater.* 2010, **22**, 1060.
- [9] (a) M. Mittal, E. M. Furst, *Adv. Funct. Mater.* 2009, **19**, 3271; (b) S. O. Lumsdon, E. W. Kaler, O. D. Velev, *Langmuir* 2004, **20**, 2108.
- [10](a) T. Ding, K. Song, K. Clays, C.-H. Tung, *Adv. Mater.* 2009, **21**, 1936; (b) M. S. Wang, L. He, Y. D. Yin, *Materials Today*, 2013, **16**, 110; (c) Q. Zhang, M. Janner, L. He, M. S. Wang, Y. X. Hu, Y. Lu, Y. D. Yin, *Nano Lett.* 2013, **13**, 1770; (d) T. Kraus, D. Brodoceanu, N. Pazos-Perez, A. Fery, *Adv. Funct. Mater.* 2013, **23**, 4529.
- [11] (a) L. Xu, H. Li, X. Jiang, J. X. Wang, L. Li, Y. L. Song, L. Jiang, *Macro. Rapid Commun.* 2010, **31**, 1422; (b) Y. Huang, M. J. Liu, J. X. Wang, J. M. Zhou, L. B. Wang, Y. L. Song, L. Jiang, *Adv. Funct. Mater.* 2011, **21**, 4436; (c) J. H. Zhang, Y. F. Li, X. M. Zhang, B. Yang, *Adv. Mater.* 2010, **22**, 4249.
- [12] (a) L. D. Zarzar, V. Sresht, E. M. Sletten, J. A. Kalow, D. Blankschtein, T. M. Swager, *Nature*, 2015, **518**, 520; (b) Y. Fang, Y. Y. Lv, F. Gong, Z. X. Wu, X. M. Li, H. W. Zhu, L. Zhou, C. Yao, F. Zhang, G. F. Zheng, D. Y. Zhao, *J. Am. Chem. Soc.* 2015, **137**, 2808; (c) X. M. Li, L. Zhou, Y. Wei, A. M. Ei-toni, F. Zhang, D. Y. Zhao, *J. Am. Chem. Soc.* 2015, **137**, 5903.
- [13](a) M. Park, C. Harrison, P. M. Chaikin, R. A. Register, D. H. Adamson, *Science* 1997, **276**, 1401; (b) B. Hua, A. Zhang, L. Li, *Angew. Chem. Int. Ed.* 2013, **52**, 12240; (c) A. J. Zhang, H. Bai, L. Li, *Chem. Rev.*, 2015, **115**, 9801.
- [14] (a) J. H. Cai, S. R. Chen, L. Y. Cui, C. C. Chen, B. Su, X. Dong, P. L. Chen, J. X. Wang, D. J. Wang, Y. L. Song, L. Jiang, *Adv. Mater. Interf.* 2015, **2**, 1400365; (b) T. Wang, S. R. Chen, F. Jin, J. H. Cai, L. Y. Cui, Y. M. Zheng, J. X. Wang, Y. L. Song, L. Jiang, *Chem. Commun.* 2015, **51**, 1367; (c) J. H. Cai, T. Wang, J. X. Wang, Y. L. Song, L. Jiang, *J. Mater. Chem.* 2015, **3**, 2445.
- [15] (a) H. B. Liu, J. L. Xu, Y. J. Li, Y. L. Li, *Acc. Chem. Res.* 2010, **43**, 1496; (b) Z. C. Wan, K. C. J. Ho, C. J. Medforth, J. A. Shelnutt, *Adv. Mater.* 2006, **18**, 2557; (c) C. Huang, L. Wen, H. Liu, Y. Li, X. Liu, M. Yuan, J. Zhai, L. Jiang, D. Zhu, *Adv. Mater.* 2009, **21**, 1721.
- [16] (a) C. S. Huang, Y. L. Li, Y. L. Song, Y. J. Li, H. B. Liu, D. B. Zhu, *Adv. Mater.* 2010, **22**, 3532; (b) H. P. Wu, H. W. Yu, Z. H. Yang, X. L. Hou, X. Su, S. L. Pan, K. R. Poepplmeier, and J. M. Rondinelli, *J. Am. Chem. Soc.* 2013, **135**, 4215; (c) Z. Xie, F. Wang, C. Y. Liu, *Adv. Mater.* 2012, **24**, 1716.
- [17](a) T. Yang, *Philos. Trans. R. Soc. London*, 1805, **95**, 65; (b) M. Liu, Z. Xue, H. Liu, L. Jiang, *Angew. Chem. Int. Ed.* 2012, **51**, 8348; (c) Z. W. Niu, J. B. He, T. P. Russell, Q. Wang, *Angew. Chem. Int. Ed.* 2010, **49**, 10052; (d) S. A. Kulnich, M. Farzaneh, *Appl. Surf. Sci.* 2009, **255**, 4056.
- [18] (a) L. Shi, J. T. Harris, R. Fenollosa, I. Rodriguez, X. T. Lu, B. A. Korgel, F. Meseguer, *Nat. Commun.* 2014, **4**, 1904; (b) Q. S. Jiang, K. Li, H. L. Wei, L. Yi, *J. Sol-Gel Sci Technol*, 2013, **67**, 565.
- [19](a) M. Kasha, H. R. Rawls, M. A. El-Bayoumi, *Pure Appl. Chem.* 1965, **11**, 371; (b) N. C. Matti, S. Mazumdar, N. J. Periasamy, *J. Phys. Chem. B.* 1998, **102**, 1528; (c) S. Gentemann, C. J. Medforth, T. P. Forsyth, D. J. Nurco, K. M. Smith, J. Fajer, D. Holtz, *J. Am. Chem. Soc.* 1994, **116**, 7363.